

# Fabrication of micro-channel arrays on thin metallic sheet using internal fluid pressure: Investigations on size effects and development of design guidelines

Sasawat Mahabunphachai<sup>a,b</sup>, Muammer Koç<sup>a,\*</sup>

<sup>a</sup> NSF I/UCR Center for Precision Forming, Department of Mechanical Engineering, Virginia Commonwealth University, Richmond, VA 23284, United States

<sup>b</sup> Department of Mechanical Engineering, University of Michigan, Ann Arbor, MI 48109, United States

Received 7 August 2007; received in revised form 5 September 2007; accepted 6 September 2007

Available online 18 September 2007

## Abstract

Micro-feature (channel, protrusion, cavity, etc.) arrays on large area-thin metallic sheet alloys are increasingly needed for compact and integrated heat/mass transfer applications (such as fuel cells and fuel processors) that require high temperature resistance, corrosion resistance, good electrical/thermal conductivity, etc. The performance of these micro-feature arrays mainly affects the volume flow velocity of the reactants inside the arrays which directly controls the rate of convection mass/heat transport. The key factors that affect the flow velocity include channel size and shape, flow field pattern, flow path length, fluid pressure, etc. In this study, we investigated these micro-feature arrays from the manufacturability perspective since it is also an important factor to be considered in the design process. Internal fluid pressure (hydroforming) technique is investigated in this study with the specific goals to, first, understand if the so-called “size effects” (grain vs. feature size) are effective on the manufacturability of thin metallic sheet into micro-channels, and second, to establish design guidelines for the micro-channel hydroforming technique for robust mass production conditions. Thin stainless steel 304 blanks of 0.051 mm thick with three different grain sizes of 9.3, 10.6, and 17.0  $\mu\text{m}$  were used in hydroforming experiments to form micro-channels with the dimensions between 0.46–1.33 and 0.15–0.98 mm in width and height, respectively. Based on the experimental results, the effect of the grain size on the channel formability was found to be insignificant for the grain size range used in this study. On the other hand, the effect of the channel (feature) size was shown to dominate the overall formability. In addition, FE models of the process were developed and validated with the experimental results, then used to conduct a parametric study to establish micro-channel design guidelines. The results from the parametric study suggested that in order to obtain the maximum aspect ratio (height-to-width ratio) a small channel width should be used. Even though a large channel width would result in a higher channel height, the height-to-width ratio was found to be lower in this case. In addition, higher aspect ratio could be obtained by using larger corner radius ( $R_d$ ), wider distance between adjacent channels ( $W_{\text{int}}$ ), or less number of channels. On the other hand, the variation in draft angle ( $\alpha$ ) between 5° and 20° in combinations with the other channel geometries was found to be insignificant on the channel formability/height. All in all, these channel parameters ( $W$ ,  $R_d$ ,  $W_{\text{int}}$ ,  $\alpha$ , channel number, etc.) should be taken into account simultaneously in the design process in order to obtain such a design of the micro-feature arrays that would meet both performance and manufacturing requirements and constraints.

© 2007 Elsevier B.V. All rights reserved.

**Keywords:** Bipolar plate; Micro-channel; Fuel cell manufacturing; Size effects

## 1. Introduction

Micro-feature (micro-channel, micro-protrusion, micro-cavity, etc.) arrays on large area-thin metallic sheet alloys are increasingly needed for compact and integrated heat/mass transfer applications that require high temperature resistance, corrosion resistance, good electrical/thermal conductivity, etc. Such applications include bipolar/interconnect plates for fuel cells (PEMFC, SOFC, MOFC), fuel reformers/processors,

\* Corresponding author. Tel.: +1 804 827 7029; fax: +1 804 827 7030.

E-mail address: [mkoc@vcu.edu](mailto:mkoc@vcu.edu) (M. Koç).

URLs: [http://www.egr.vcu.edu/me/faculty/me-faculty\\_koc.html](http://www.egr.vcu.edu/me/faculty/me-faculty_koc.html) (M. Koç), <http://www.CPForming.org> (M. Koç).

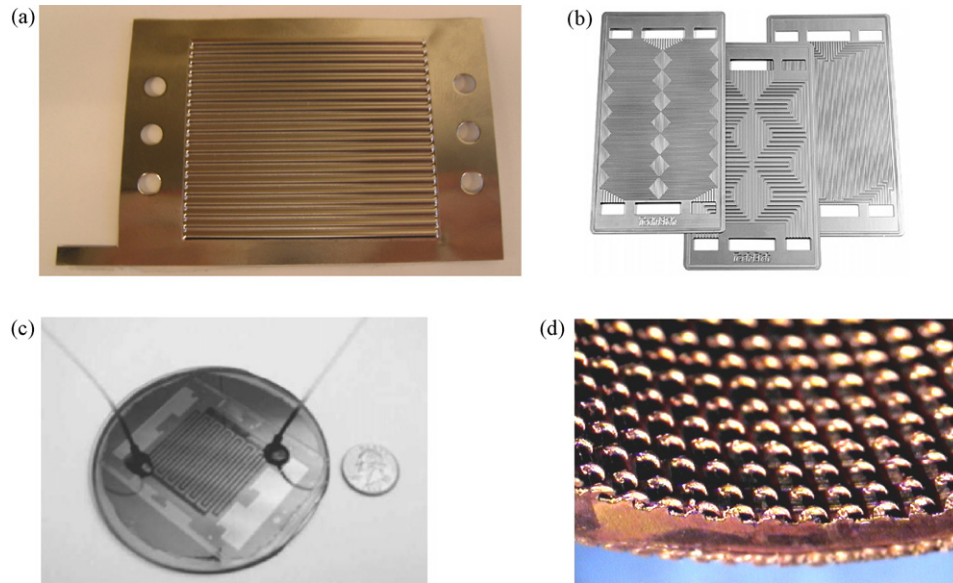


Fig. 1. Micro-feature arrays on thin metallic sheet for (a and b) PEM fuel cell, (c) micro-reactor, and (d) micro-heat exchanger applications.

micro-power generators, micro-reactors, micro-heat exchangers, micro-turbines, etc. (Fig. 1). Apparently, channel geometry, size, and configuration have a great influence on the ultimate functionality of the channel arrays such as mass transportation and heat transfer [1,2]. For example, the hydrogen consumption level at the anode of the PEMFC could be enhanced by choosing appropriate channel dimensions (i.e. width, height, land/spacing) and shapes (e.g. hemispherical, triangular, and rectangular shapes), flow field pattern (e.g. serpentine, interdigitated, and spiral-interdigitated), flow path length, fluid pressure, etc. [1–3]. In general, the ideal micro-channels for heat/mass transfer applications should provide (i) a maximum volume flow rate of reactants to increase convection heat/mass-transport, (ii) a uniform distribution of reactants and temperature, and (iii) a small pressure drop (minimize parasitic losses). However, in a recent study by Feser et al. showed that a large pressure drop across a single-serpentine flow field may also enhance the ability of the cell to remove liquid water and carbon dioxide bubble blockages produced on the cathode and anode sides of direct methanol fuel cells (DMFCs), respectively [4]. In addition, effective water removal in the PEMFC also requires a rational design of the flow channels taken into account both performance and durability issues [3,5,6].

In this study, we focused our investigations on the manufacturability of such micro-feature arrays to determine the limitations and challenges of making micro-channels with desired size, shape and distribution for given application. Examples of existing manufacturing methods of micro-feature arrays on thin metallic sheet alloys include (a) stamping of stainless steel sheets as shown in Fig. 1a [7], (b) photo etching of stainless steel/titanium plates as shown in Fig. 1b [Tech-etch, Inc.], (c) Lithography Galvanik Abformung (LIGA) with electroforming of stainless steel plate [8], and (d) hydroforming of pure copper (3.0  $\mu\text{m}$  thick) and stainless steel (AISI304, 2.5  $\mu\text{m}$  thick) foils [9].

With several advantages in terms of simple process setup, surface topology, thickness distribution, and maximum formability of the final parts under the bi-axial loading and frictionless conditions, hydroforming of thin metallic sheet alloys stands out as a prominent candidate to be used in a large-scale production of the micro-feature arrays. Therefore, in this study we investigated the hydroformability of micro-channels. However, as in any micro-manufacturing processes, the so-called “size effects” on the material behavior, and thus manufacturability, have been known to exist [10,11]. Therefore, in the first part of the study, the “size effects” were investigated to understand if and to what extent they affect the formability of thin metallic sheet into micro-channels. Hydroforming experiments were conducted using thin stainless steel 304 blanks of 0.051 mm thick with different grain sizes into several channel geometries. In the second part, we focused our study on the establishment of design guidelines for the micro-channel hydroforming technique for robust mass production conditions through a set of parametric studies.

In the following two sections, hydroforming experimental setup and conditions are presented, followed by the discussion of the experimental results. In Section 4, we presented the finite element analysis (FEA) that were developed and validated with the micro-channel experiments based on several material flow curves obtained from hydraulic bulge tests. In Section 5, the validated FE models were used to conduct a parametric study to establish design guidelines. These design guidelines are expected to minimize the trial-and-error procedures when designing and fabricating micro-channel array devices to result in optimal dimensions or shapes for different applications.

## 2. Experimental setup

An experimental apparatus for thin sheet hydroforming was developed as shown in Fig. 2. The setup is composed of an upper die (1) that has an opening at the middle with a shoulder to allow

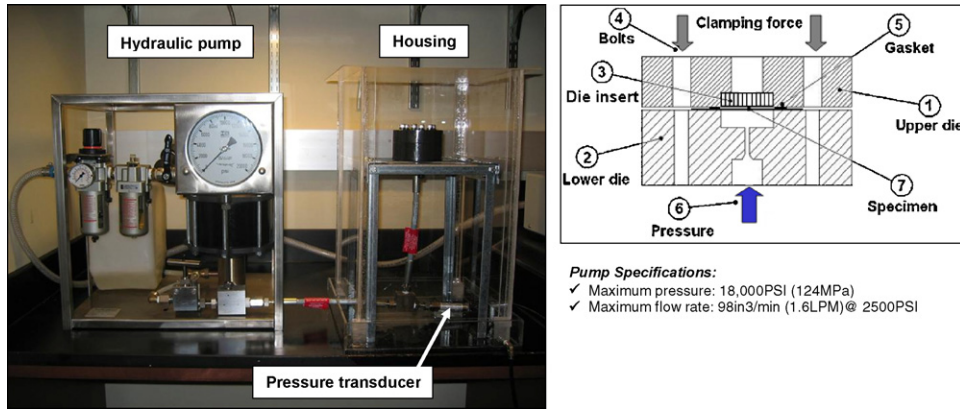


Fig. 2. Hydroforming process apparatus.

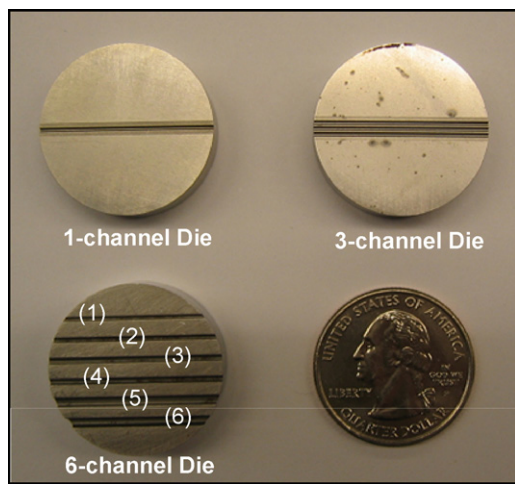


Fig. 3. Die inserts: 1-channel, 3-channel, and 6-channel dies.

the use of different die inserts (3), a lower die (2) that has an opening at the bottom for the pressure injection, threaded bolts (4) to provide clamping force, and copper gaskets (5) to provide sealing. Three different micro-channels die inserts, namely 1-channel die, 3-channel die, and 6-channel die as shown in Fig. 3, with channel dimensions between 0.46 and 1.33 mm in width, and 0.15–0.98 mm in height, were used in this study. Detailed geometries of the micro-channels on each die insert could be found in Table 1. The forming pressure was measured and recorded using a pressure transducer (Omega PX605), while the formed micro-channel profiles were measured using a laser sensor (Keyence LK-G37) that has high accuracy of 0.05  $\mu\text{m}$  (Fig. 4).

### 3. Experimental results and discussion

The first set of the hydroforming experiments were performed on thin blanks of SS304 in the as-received condition (grain size = 10.6  $\mu\text{m}$ ) using all three die inserts to evaluate the process repeatability and the laser measurement accuracy. Samples of hydroformed micro-channels are shown in Fig. 5 and the micro-channel profiles measured using the laser sensor for different specimens formed at different pressure levels of 55.2 and

Table 1  
Micro-channel geometries on different die inserts

Feature	Dimensions of each die insert (mm)							
	1-Channel	3-Channel	6-Channel					
			#1	#2	#3	#4	#5	#6
$W$	0.46	0.46	0.52	0.63	0.78	0.78	1.33	1.33
$H$	0.50	0.50	0.15	0.24	0.24	0.46	0.46	0.98
$R_d$	0.13	0.13	N/A	N/A	N/A	0.13	0.26	0.26
$B$	0.11	0.11	N/A	N/A	N/A	N/A	N/A	N/A
Channel spacing <sup>a</sup>	N/A	0.82	3.00	3.00	3.00	3.00	3.00	3.00

All channels have 10° draft angle.

<sup>a</sup> Distance measured from center to center of adjacent channels.

82.7 MPa (8,000 and 12,000 psi) are presented in Fig. 6. The measurement results showed good process repeatability on all three die inserts with a maximum variation in the channel height of less than 20  $\mu\text{m}$  and the variation in laser measurement val-

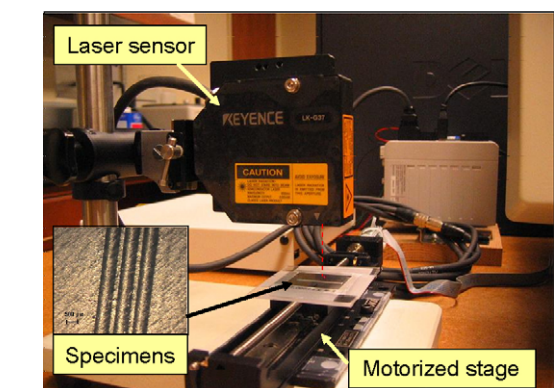


Fig. 4. Laser measurement system (Keyence LK-G37 laser sensor).



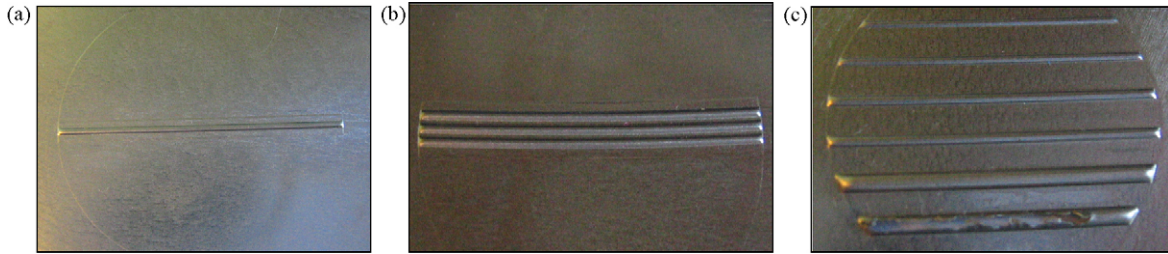


Fig. 5. Samples of hydroformed micro-channels on SS304, 0.051 mm thick. (a) Single-channel specimen, (b) 3-channel specimen, and (c) 6-channel specimen.

ues between different runs of the same location were found to be less than 1  $\mu\text{m}$ .

The effect of the pressure was clearly shown in the 1-channel and 3-channel samples where higher channel height ( $h$ ) was obtained at higher pressure level. The effect of channel spacing, defined as the distance measured from center to center of adjacent channels (a.k.a. inter-channel distance,  $W_{\text{int}}$ ), was also observed in the case of using the 1-channel and 3-channel dies where less formed height was measured from the 3-channel specimens due to the more constraint on the material flow. On the other hand, the formed height on the 6-channel specimens appeared to be more dependent on the die width ( $W$ ) rather than the die height ( $H$ ) or pressure. For example, higher channel height ( $h$ ) was obtained when wider channel was used

( $W = 1.33 \text{ mm}$  for channel #5 and  $W = 0.78 \text{ mm}$  for channel #4, both with  $H = 0.46 \text{ mm}$ ). In addition, the channel heights ( $h$ ) were measured to be approximately same in the case of forming channel #3 and #4 that have different die height ( $H$ ), but the same die width ( $W$ ), showing the dominant effect of the die width ( $W$ ) on the formability over the die height ( $H$ ). Another notable observation was also made in forming channel #5 and #6, both with  $W = 1.33 \text{ mm}$ , but different die height ( $H$ ). At the pressure level of 82.7 MPa (12,000 psi), the blanks were ruptured in channel #6, while a fully formed channel was obtained in channel #5. This observation suggested that there exists an optimal aspect ratio ( $h/W$ ) that could be obtained at each specific pressure level above which rupture could occur due to excessive wall thinning.

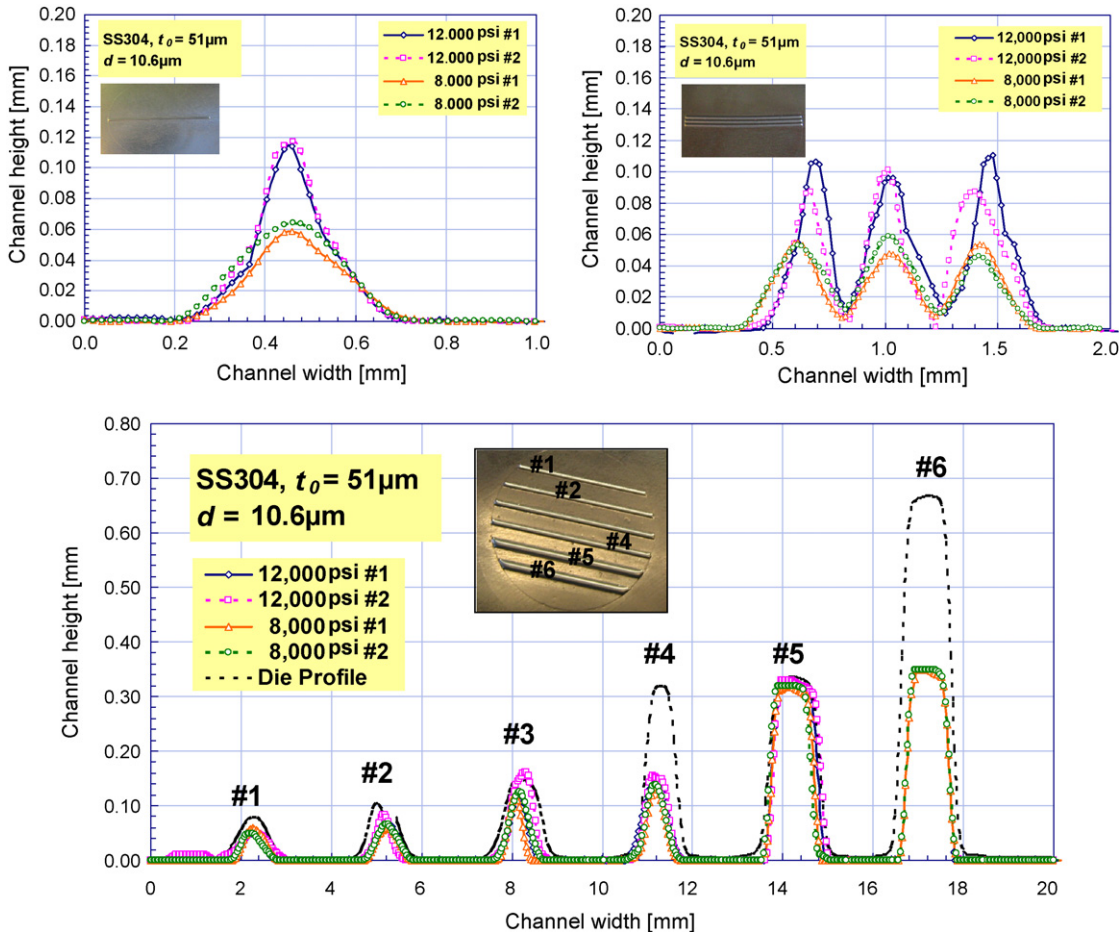


Fig. 6. Micro-channel profiles of 1-channel (top left), 3-channel (top right), and 6-channel (bottom) specimens.

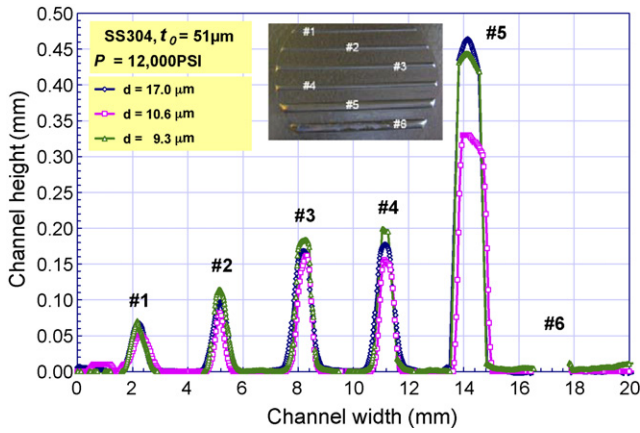


Fig. 7. Effect of material grain size on the micro-channel formability.

In the second set of experiments, the effect of the material grain size was investigated by using thin SS304 blanks with three different grain sizes ( $d=9.3, 10.6,$  and  $17.0 \mu\text{m}$ ). These blanks were hydroformed using 6-channel die at a pressure level of 82.7 MPa (12,000 psi). The hydroformed channel profiles are shown in Fig. 7. The measurement profiles showed an uncertain trend of the grain size effect on the channel height/formability; therefore, no conclusion could be drawn at this time. In addition, the process variation of about  $20 \mu\text{m}$  as discussed previously is also believed to contribute to the differences in the channel height values. Finally, channel #6 was also found to rupture for all three grain sizes at this pressure level.

To consider the in-plate variation of the channel dimensions, a pair of CCD cameras (GOM ARAMIS System by Trilion) was used to obtain the micro-channel profiles at different locations (Sections 1–3) as shown in Fig. 8. With the ARAMIS system, the specimen was required to be spray painted for the analysis reason. Even though the paint layers ( $\approx 60 \mu\text{m}$ ) could affect the actual dimensions of the micro-channels, this measurement method could serve the purpose of the in-plate variation study well given that the spray painting was deposited evenly on the specimen surface. Fig. 9 illustrated the channel profiles of the specimen formed using the 3-channel die at 82.7 MPa. The in-plate variation was found to be less than  $5 \mu\text{m}$  in both the width and the height dimensions.

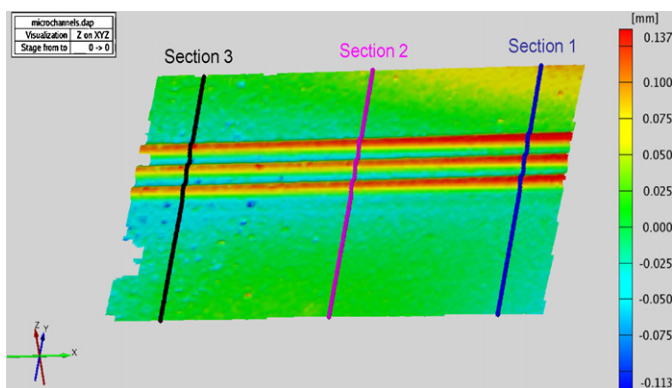


Fig. 8. In-plate variation study using CCD cameras.

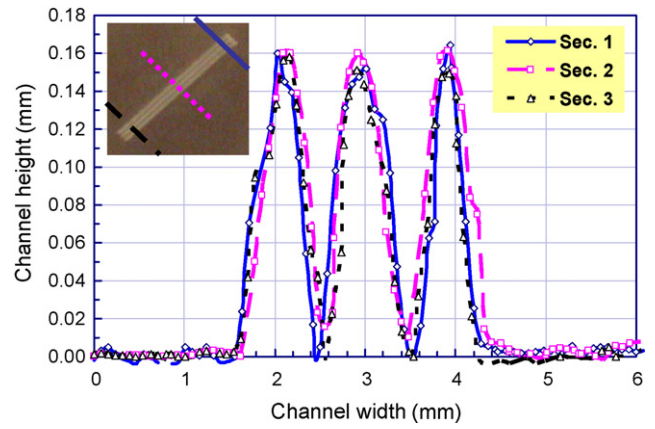


Fig. 9. In-plate variations plot.

In this section, the experimental results showed that the process is repeatable and the measurement system is accurate. Both in-plate and between-plate variations were found to be in a reasonable range of 5 and  $20 \mu\text{m}$ , respectively; thus, the process was shown to be robust and suitable for producing accurate micro-channel dimensions to be used in micro-devices. In the following section, FE models were developed and validated with the experimental results.

#### 4. FE models and validation

The hydroforming process of thin sheet blanks to form micro-channel arrays is modeled using an FE tool (MSC.Marc) to further investigate the manufacturability of different micro-channel designs. One of the crucial factors leading to reliable process and design predictions is the use of accurate material models. In order to obtain the material properties, the same thin SS304 blanks were bulged using three different bulge diameters of 10, 20, and 100 mm and the material flow curves of the blanks were calculated. These material flow curves are used as the material models in a reversed FEA study to simulate the micro-channel hydroforming process. The material constants that described the flow curves ( $\sigma = K\epsilon^n$ ) for different bulge diameters are presented in Table 2 for the as-received material ( $d=10.6 \mu\text{m}$ ). Other material data used in the model were Young’s modulus of 195 GPa, Poisson’s ratio of 0.29, and mass density of  $8\text{E-}9 \text{ kg m}^{-3}$ . Based on the experimental and simulation result comparisons, the material flow curve or model that best describe the material behavior of the thin SS304 blanks in the hydroforming process will be selected to be used in the next section where a series of parametric studies is conducted.

Table 2  
K and n values from bulge tests for different bulge diameters

SS304, $t_0 = 51 \mu\text{m}$ , $d = 10.6 \mu\text{m}$	Bulge diameter, $D_c$ (mm)		
	10	20	100
K (MPa)	1329	1246	1266
n	0.72	0.49	0.47

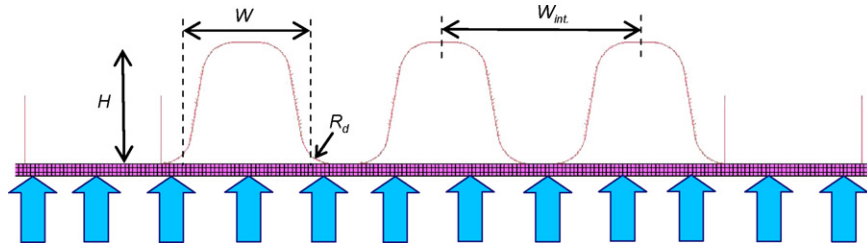


Fig. 10. Simulation setup.

As for the boundary and loading conditions of the FE models, the blank is fixed at the nodes at both ends to prevent the draw-in effect, and normal pressure was applied at the element edge as illustrated in Fig. 10. A ramp pressure loading with a slope of 2,000 psi/s was selected based on the actual pressure profile measured during the experiments. Solid elements were used for the modeling of the blank with three to eight elements across the thickness depending on the maximum strain value in each case. Coulomb friction condition was assumed with a friction coefficient of 0.03. The FE model of the process setup is demonstrated in Fig. 10 for the 3-channel die insert.

The simulation results are compared with the experimental measurements in Fig. 11. The comparisons of the results showed poor predictions of the channel hydroformability for all material flow curves obtained from different bulge sizes. The poor predictions are believed to be caused by the feature size effect on the

material response. Since there is a significant difference in size scales between the bulge diameters ( $D_c = 10, 20, \text{ and } 100 \text{ mm}$ ) and the micro-channel width ( $W = 0.5 \text{ mm}$ ), the flow curves calculated based on the material response during the bulge tests may not represent the actual deformation mechanics of the same material blanks in the micro-channel hydroforming; and thus resulted in the discrepancy in the result comparisons.

The variations in the dome height values for the 3-channel die as shown in Fig. 11 were calculated based on the differences between the height of the middle and left/right channels where lower channel height is obtained at the middle channel due to more constraints on the material flow as illustrated in Fig. 12.

Finally, since the flow curves obtained from the macro/meso-scale bulge testing could not represent the material behavior in the micro-channel hydroforming process, a reversed engineering method was utilized with an attempt to capture the material flow curve that would yield better predictions in terms of the channel formability as compared to the experimental results. Based on different trial and error runs in the FEA, the flow curve with  $K = 1400 \text{ MPa}$  and  $n = 0.12$  yielded the channel height predictions for both the 1-channel and 3-channel dies within an acceptable range as shown in Fig. 13, and thus, will be used in the parametric study to investigate the effects of other channel design parameters to establish design rules for the micro-channels.

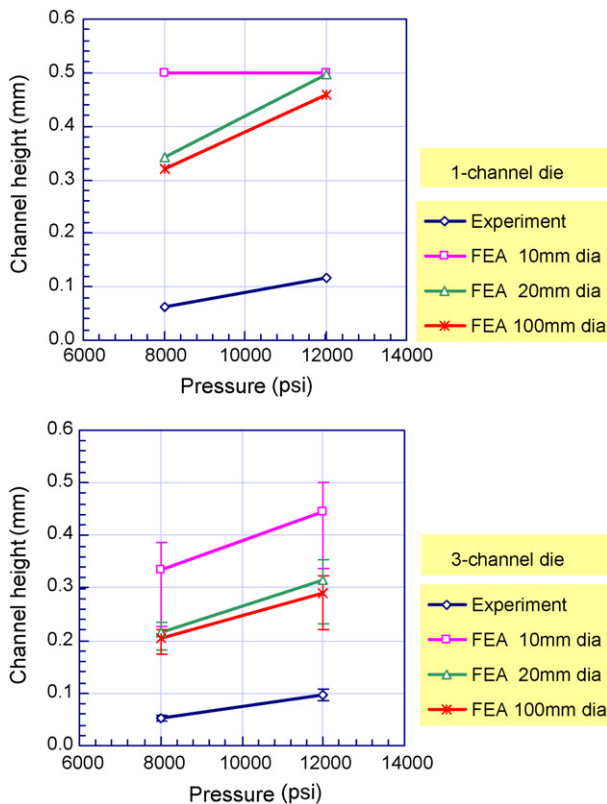


Fig. 11. Simulation results for 1-channel die and 3-channel die using different material flow curves obtained from different bulge diameters.

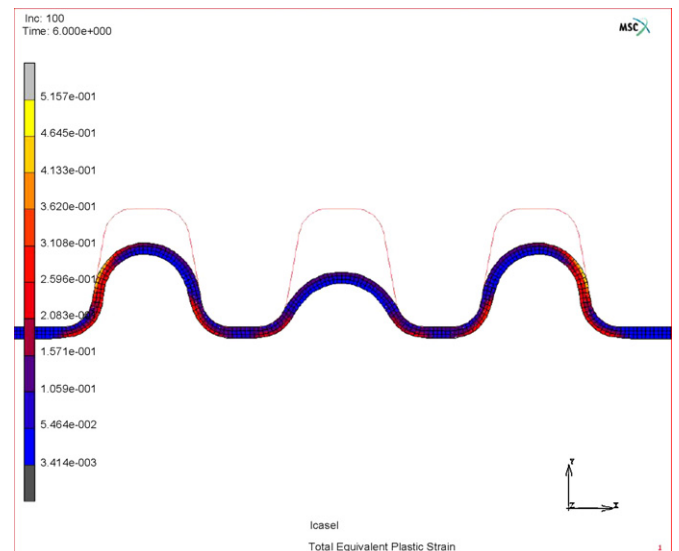


Fig. 12. Simulation result of 3-channel die.



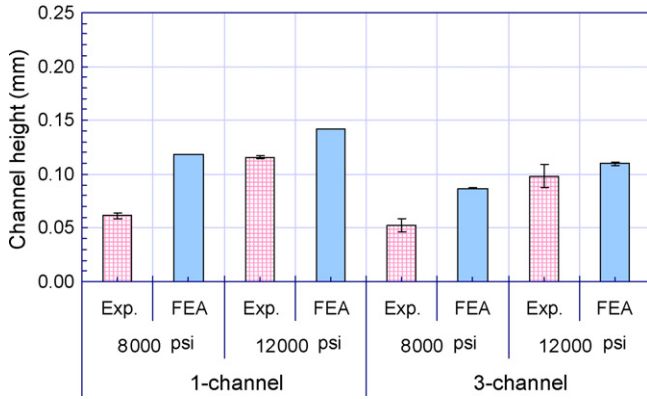


Fig. 13. Reversed engineering:  $\sigma = K\epsilon^n$  with  $K = 1400$  MPa and  $n = 0.12$ .

**5. Parametric study**

In this section, a parametric study is conducted using the validated FE to investigate the effect of different micro-channel geometries on the overall formability. The studied parameters include die width ( $W$ ), draft angle ( $\alpha$ ), die corner radius ( $R_d$ ), channel spacing (i.e. inter-channel distance,  $W_{int}$ ), and channel number. The channel height ( $h$ ) is regarded as the output response from the simulation to represent the formability; and thus, the channels on the die are modeled such that the bottom part is open (Fig. 14). Furthermore, the initial blank thickness ( $t_0$ ) was kept constant at 0.051 mm for all simulation cases since we only knew the material properties of the SS304 blanks at this thickness from the bulge tests. Nonetheless, since the formability of the channel depends on the ratios of the channel geometries to the blank thickness (i.e.  $W/t_0$ ,  $R_d/t_0$ ,  $W_{int}/t_0$ , etc.) rather than each individual parameter, we could also understand the effect of changing in thickness by varying other channel parameters itself. The parametric study was divided into two sections: single-channel and multi-channel hydroforming. In the former, the effect of the channel width ( $W$ ), draft angle ( $\alpha$ ), and die corner radius ( $R_d$ ) were investigated, while the latter focused on the effect of the inter-channel distance ( $W_{int}$ ) and channel number.

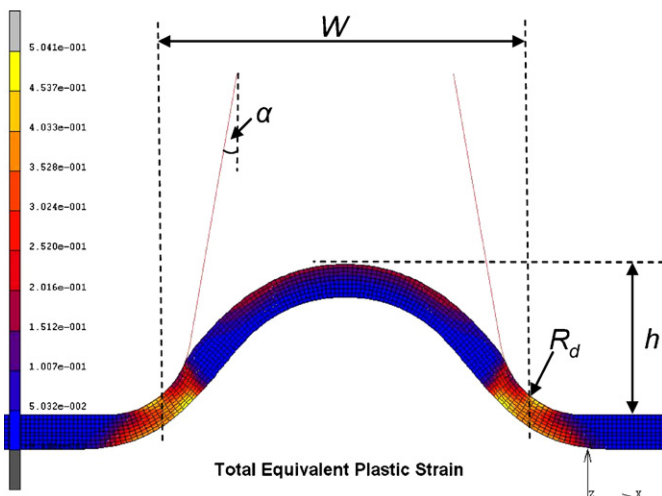


Fig. 14. Studied parameters in the FE simulations.

Table 3  
Study cases of single-channel in FEA

Studied parameters	$W$ (mm)	$\alpha$ ( $^\circ$ )	$R_d$ (mm)
Die width, $W$	0.125, 0.25, 0.5, 1.25, 2.5	10	0.125
Draft angle, $\alpha$	0.5	5, 10, 20	0.125
Die corner radius, $R_d$	0.5	10	0.0625, 0.125, 0.25

**5.1. Single-channel hydroforming**

The studied ranges of  $W$ ,  $\alpha$ , and  $R_d$  are given in Table 3. For each case, the blank was hydroformed up to the maximum pressure ( $P_{max}$ ) level, defined as the pressure level where the maximum thickness reduction is 25% of the initial thickness (i.e. 25% thinning). The aspect ratio (AR), defined as the ratio between the formed height ( $h$ ) and the channel width ( $W$ ), was used as the formability index. The simulation results are presented in Fig. 15.

The simulation results showed that higher aspect ratio could be obtained when smaller channel width was used. The width

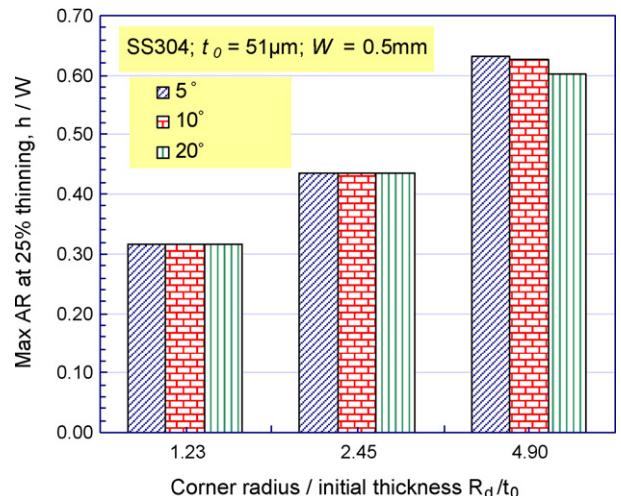
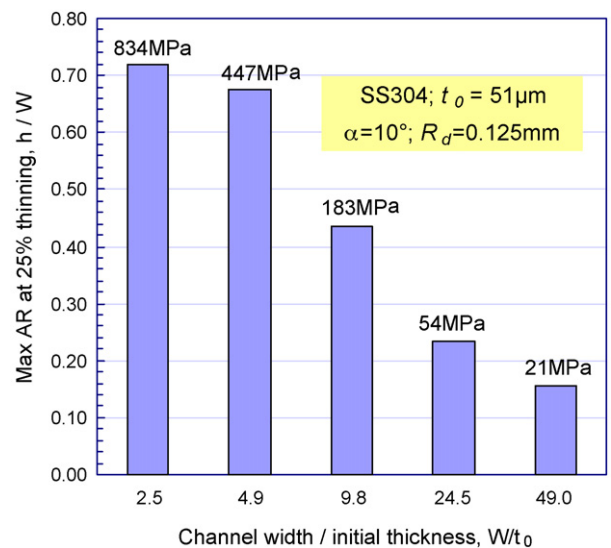


Fig. 15. Effect of channel width ( $W$ ), corner radius ( $R_d$ ), and draft angle ( $\alpha$ ) on maximum aspect ratio (AR).

of the channel could be reduced as low as 2.5 times of the initial thickness based on the simulation results. However, very high pressure levels were required to obtain such a high aspect ratio; thus, increases the setup cost and cycle time in the production. Therefore, the suggested micro-channel design, compromising both aspect ratio and pressure level, is suggested to be between  $W/t_0$  of 5 and 10. Note that higher aspect ratio could be obtained if more thinning is allowed. Alternatively, the aspect ratio could also be increased by increasing the corner radius ( $R_d$ ). For example, by increasing  $R_d$  value from 0.0625 to 0.25 mm, about 90% increase in AR was observed. Therefore, large values of corner radius are recommended to be used to improve the overall formability. Nonetheless, the size of  $R_d$  should be carefully selected to optimize the number of channels that can be produced on a given plate size. On the other hand, the effect of the draft angle ( $\alpha$ ) in combination with other channel geometries used in this parametric study was shown to be insignificant. Therefore, the draft angle is suggested to be made as low as possible to maximize the cross-sectional area of these channels in order to reduce the pressure drop value, and thus, increase the heat/mass transfer capability.

### 5.2. Multi-channel hydroforming

The effects of channel spacing ( $W_{int}$ ) and channel number on the height and thickness variation are investigated using FEA

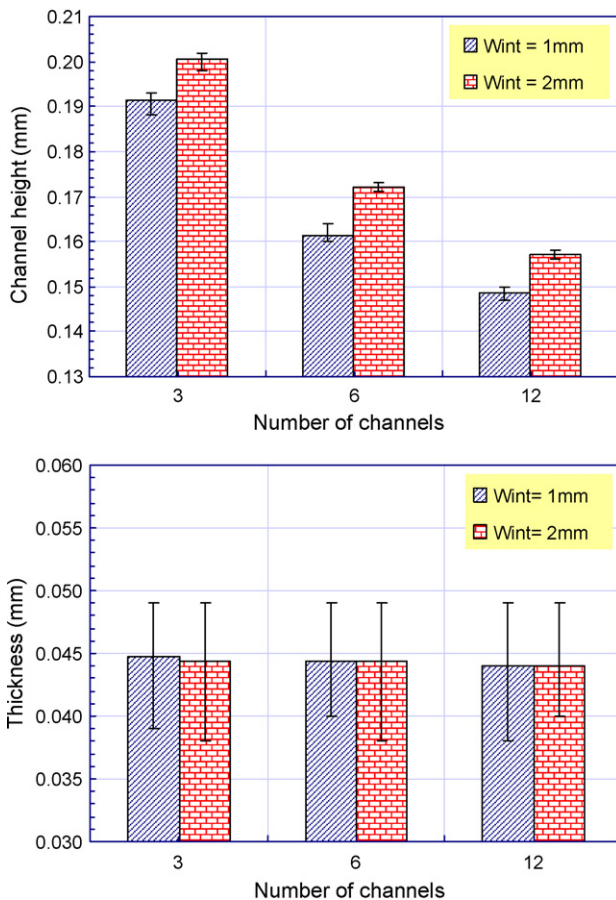


Fig. 16. Effect of channel spacing ( $W_{int}$ ) and channel number on the channel height and thickness distribution.

in this section. The selected ranges for the channel spacing and the channel number were 1–2 mm and 3–12, respectively. The simulations were also stopped at 25% thinning. Other parameters were kept constant as follows: channel width ( $W$ ) = 0.5 mm, draft angle ( $\alpha$ ) =  $10^\circ$ , corner radius ( $R_d$ ) = 0.125 mm, and the initial blank thickness ( $t_0$ ) = 0.051 mm. The simulation results were presented in the diagrams in Fig. 16.

Both channel spacing and channel number were shown to have considerable impact on the channel hydroformability. Higher channels could be formed when using larger channel spacing or less number of channels. On the other hand, only slight effect of these two parameters was observed on the thickness distribution. The thinnest location was observed at the corner radius of the channel close to, but not at, the channel at the middle of the arrays. The thickness at the land and valley regions for all studied cases here was measured to be 0.049 mm. In other words, the upper bound of the thickness variation showed in Fig. 16 was measured at the land or valley regions, while the lower bound was measured at the corner radius areas.

## 6. Summary and conclusions

In this study, the fabrication of micro-channels using internal fluid pressure (hydroforming) was investigated emphasizing on the design and manufacturability issues. A hydroforming apparatus was developed to conduct micro-channel hydroforming experiments on thin SS304 sheets (51  $\mu\text{m}$  thick) with different material grain sizes (9.3–17.0  $\mu\text{m}$ ). The repeatability of the process and the accuracy of the laser measurement system were first evaluated and shown to be reliable with small variations of in-plate and between-plate channel dimensions below 5 and 20  $\mu\text{m}$ , respectively. The experimental results showed unclear effect of the material grain size, but significant impacts of the forming pressure and the feature (channel) size on the channel formability/height.

FEA tool was employed to conduct a parametric study to establish design guidelines for the micro-channels in the hydroforming process. The studied parameters were channel width ( $W$ ), draft angle ( $\alpha$ ), die corner radius ( $R_d$ ), channel spacing ( $W_{int}$ ), and channel number. The material flow curve used in the parametric study was obtained from reversed engineering of the experimental results in the FEA because none of the material flow curves calculated from the bulge tests with different bulge diameters (10, 20, and 100 mm) did not provide accurate predictions of the channel height. The results from the parametric study suggested that in order to obtain the maximum channel aspect ratio ( $AR = h/W$ ), a small channel width ( $W$ ) should be used. Even though a large channel width ( $W$ ) would result in a higher channel height ( $h$ ), the aspect ratio ( $h/W$ ) was found to be lower in this case. In addition, higher aspect ratio could be obtained by using larger corner radius ( $R_d$ ), wider channel spacing ( $W_{int}$ ), or less number of channels on a given plate size. In this study, the variation in draft angle ( $\alpha$ ) between  $5^\circ$  and  $20^\circ$  in combinations with the other channel geometries was found to be insignificant on the channel height. On the other hand, the thickness reduction on the multi-channel arrays was found to be about 4% at the valley and land locations, while around



25% thinning was observed at the corner radius regions. All in all, these channel parameters ( $W$ ,  $R_d$ ,  $W_{int}$ ,  $\alpha$ , channel number, etc.) would need to be designed and optimized simultaneously in order to obtain such a design of the micro-feature arrays that would meet the performance requirements and still be within the manufacturing limitations.

In the near future, we will attempt to fabricate actual size bipolar plates (e.g. 10 cm  $\times$  10 cm) on thin SS304 blanks using the hydroforming technique and conduct performance tests of these bipolar plates in a single and multi-stack fuel cell test systems. The channel geometries and flow patterns on these bipolar plates will be designed based on further FEA results of the large area bipolar plates and several design recommendations as suggested in the literatures for optimum performance. Finally, more material tests (bulge test) at the micro/meso-scales are strongly recommended in order to obtain material data that is more accurate which, in turn, will result in reliable process/channel design and optimization in FEA.

## References

- [1] R.G. Kumar, G. Reddy, J. Power Sources 113 (2003) 11–18.
- [2] S.W. Cha, R. O'Hayre, Y. Saito, F.B. Prinz, J. Power Sources 134 (2004) 57–71.
- [3] X. Li, I. Sabir, J. Park, J. Power Sources 163 (2007) 933–942.
- [4] J.P. Feser, A.K. Prasad, S.G. Advani, J. Power Sources 161 (2006) 404–412.
- [5] P. Quan, B. Zhou, A. Sobiesiak, Z. Liu, J. Power Sources 152 (2005) 131–145.
- [6] A.A. Shah, G.-S. Kim, W. Gervais, A. Young, K. Promislow, J. Li, S. Ye, J. Power Sources 160 (2006) 1251–1268.
- [7] J.P. Allen, Proceedings of the Fuel Cell Seminar Abstracts, 2000, pp. 55–58.
- [8] S.-J. Lee, Y.-P. Chen, C.-H. Huang, J. Power Sources 145 (2005) 369–375.
- [9] B.Y. Joo, S.I. Oh, Y.K. Son, CIRP Ann. 53 (1) (2004) 243–246.
- [10] T.A. Kals, R. Eckstein, J. Mater. Process. Technol. 103 (2000) 95–101.
- [11] M. Geiger, M. Kleiner, R. Eckstein, N. Tiesler, U. Engel, Ann. CIRP, 50 (2) 2001, pp. 445–462 (Keynote paper).